Methodology for Broadband Matching of Electrically Small Antenna using combined Non-Foster and Passive Networks

Saadou Al Mokdad, Raafat Lababidi, Marc Le Roy, Sawsan Sadek, André Pérennec, Denis Le Jeune

Methodology for Broadband Matching of Electrically Small Antenna using combined Non-Foster and Passive Networks

Saadou Almokdad[1,2], Raafat Lababidi[1], Marc Le Roy[1], Sawsan Sadek[3], André Pérennec[1], Denis Le Jeune[1]

Abstract
Decreasing the electric length of an antenna results in increasing its input reactance that becomes greater than its input resistance, resulting in a significant rise in its quality factor and in a drastic reduction of its potential operating bandwidth. For such small antennas, namely ESA for Electrically Small Antenna, passive matching is restricted by the gain-bandwidth theory, providing narrow bandwidths and/or poor gain. This limitation can be overtaken by using antenna matching networks based on non-Foster components. In previous studies, non-Foster components are used to cancel the reactance part of the ESA, and then passive matching may be introduced to transform the net input impedance toward 50Ω, which leads to an increase in the bandwidth. In this paper, a design methodology is put forward on three different topologies all based on combined passive and active matching networks. A described step-by-step design to decrease the antenna quality factor is discussed. A comparison is made between these topologies along with a discussion on their limitations and ability to increase the bandwidth and radiation efficiency of ESA. The third topology presented in this paper is a novel one that proposes a three-stage matching network and exhibits both the widest matched bandwidth and an increase in the efficiency of the whole system compared to previous approaches. In order to make this comparison, a new indicator to estimate the whole system radiated power efficiency is introduced and validated by comparison with a full EM simulation. Moreover, actual implementation of the two most interesting techniques are detailed and associated measured results are carefully compared to simulations.

Keywords Non-Foster, passive matching, quality factor, electrically small antenna

1 Introduction

The demand for wide-band small antennas is steadily increasing for future wireless communication systems, due to the need of compact multi-function and multi-standard devices. Electrically Small antennas (ESA) are thus required due to the limited space available in the structures such as electronic mobile devices (5G), IoT (Internet of Things), medical equipment, etc. However, practical application in today's electronic systems is limited by their fundamental tradeoff between bandwidth and efficiency using passive impedance matching techniques [1]. Non-Foster Circuits (NFCs) are active circuits that promise to break the fundamental tradeoffs between size, operating frequency and bandwidth for electrically small antennas [2], [3].

✉ Saadou AlMokdad
Saadou-ali-almokdad@hotmail.com

[1] Lab-STICC (UMR CNRS 6285), UBO, ENSTA-Bretagne, Brest, France
[2] Doctoral School of Science and Technology, Lebanese University, Hadath, Lebanon
[3] Faculty of Technology, Lebanese University, Saida, Lebanon

An antenna is considered to be an ESA when it satisfies the following condition: k.a < 0.5, where k is the wave number and a is the radius of a hypothetical sphere enclosing the antenna [4].

Furthermore, ESAs famously suffer from high quality factor Q because of their high reactance value compared to their small resistive value, resulting in storing the input power in their near field and a small portion radiates in their far field [5]. Wheeler and Chu [6] have provided detailed descriptions of the fundamental trade-off between efficiency-matched bandwidth for ESA when using passive matching networks. This limitation relies strongly on the quality factor Q, defined in Equation (1) as the ratio of the antenna reactance over its resistance:

$$Q = \frac{|X|}{R} \tag{1}$$

A high Q affects the antenna matching as illustrated by calculating the return loss S_{11} at the antenna input terminals:

$$S_{11}(dB) = 10 Log \frac{([R(\omega)-Z_0]^2+X(\omega)^2)}{([R(\omega)+Z_0]^2+X(\omega)^2)} \tag{2}$$

Where the antenna input impedance is $Z = R(\omega) + j.X(\omega)$ and reference port impedance Z_0 equals to 50 Ω. For large values of $X(\omega)$, the return loss S_{11} approaches one and the reflected power at the antenna input increases considerably. Consequently, outcomes from various methods have to be evaluated in order to identify the most relevant approach that allows to decrease the reactive part of the antenna input

reactance X(ω). Using only passive matching will lead to efficiency-bandwidth trade-off i.e. wideband matching is achieved by incorporating loss in the circuit, in other words, the efficiency of power-transfer to and from the antenna will be prohibitively weak. The maximum achievable bandwidth using only passive elements is bounded by the Bode-Fano limit [7], [8], which is summarized in [9]. This limit can be overcome by using Non-Foster active matching (i.e. negative capacitance or inductance) [10], [11], which is characterized by a negative reactance characteristics.

Our study is based on using non-Foster elements along with passive matching in order to decrease the antenna Q factor, and to increase the bandwidth as well as the radiation efficiency of the antenna. Matching the antenna at lower frequency results in shifting down its operating frequency, i.e. making the antenna electrically small. Many previous papers have already described the use of non-Foster to cancel the antenna reactance, where a passive matching circuit is also associated to transform the antenna real part toward 50Ω [10]. Another understudy topology consists on focusing first to transfer the antenna real part towards 50Ω then canceling the reactive part using non-Foster network.

The main significant contributions of this paper are as follows:

i) The use of Non-Foster elements to improve the wideband matching compared to passive elements is evidenced and a step-by-step guideline of both techniques described above is given.

ii) Then, a novel third topology that gives better performances in terms of matching bandwidth and efficiency is introduced and compared to reference topology. In addition, a comparison is carried out between the three topologies in term of bandwidth and efficiency. Our proposed topology uses first a passive network to decrease the quality factor of the antenna by increasing its resistive part, and then uses NF elements to cancel the reactive part and finally passive network again to transfer it to 50Ω.

iii) As few papers have dealt with efficiency in non-Foster matched ESA, we put forward a new indicator named TTC (Total Transmission Coefficient) specifically introduced to easily and quickly estimate the whole system efficiency (antenna + matching network). This indicator relevance and the systems efficiency is validated through co-simulations of circuit and full-EM simulations. The efficiency is found to be the next milestone to overcome in such active ESA.

Finally, prototyping and measurements of the two most interesting approaches are described and a thorough comparison of simulated and experimental results is also presented, discussed and compared to previous works [10].

2   Antenna Matching Theory

2.1   Conventional Monopole Antenna

Our case study rely on a planar monopole antenna, which is designed and simulated by CST software to resonate initially at 2.3 GHz. The antenna schematic and its simulated return loss are presented in Figure 1, while the antenna impedance simulation responses are given in Figure 2. We can notice that the antenna has a high Q factor, where the reactance value are high compared to the real value which is small for Ka < 0.5; (a is the minimum radius of the radian sphere that covers the monopole antenna and is here equal to 12.5mm, the antenna is considered ESA for frequencies below 1.9 GHz). The antenna is implemented on a 0.81 mm thick Rogers RO4003c (ε_r = 3.55, tan (δ) = 0.0027) dielectric substrate with 0.035 mm thick copper metallization, the main dimensions of the printed monopole can be seen in Figure 1.

Our goal focuses on decreasing the operating frequency to around 1.6 GHz (i.e. creating an ESA with Ka = 0.4), and on increasing its bandwidth by using several combinations of passive and NF matching techniques while verifying the matched antenna efficiency. Indeed, here we choose to match the antenna around 1.6 GHz (i.e. Ka = 0.4) because at lower frequencies the antenna has a so small radiation efficiency (Figure 3), so it will be difficult to get a satisfactory efficiency below that frequency whatever the matching network.
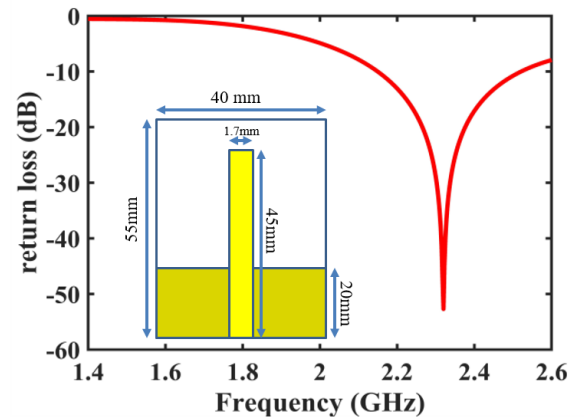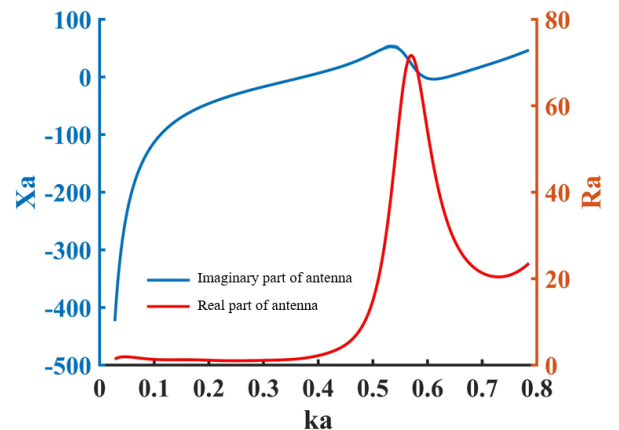

Fig. 1 Antenna schematic and return loss

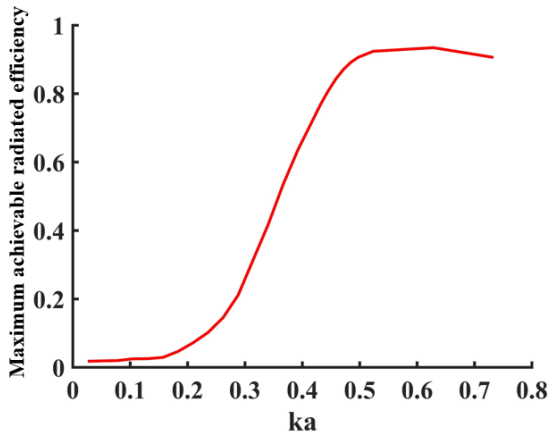**Fig.2** Antenna impedance (real and imaginary) parts

Fig. 3 Maximum achievable antenna radiation efficiency

2.2 Passive and non-Foster matching basics

First, let's recall the basics for passive matching method by considering the task of matching the impedance of an ESA to a constant value R (typically 50Ω). With high-Q antenna, such goal is difficult to achieve because of the constraints imposed by the gain-bandwidth theory of Fano [8], Bode [7]. The simplest impedance transformation network is the L-network, which requires only two reactive components, either a high pass or a low pass filter. To increase the bandwidth of the system one must decrease the Q factor which can be done by cascading L-networks in series [9] as shown in Figure 4, where the Q factor of a 5Ω load is lowered by cascading two L-networks compared to using one L-network, which leads to a wider matching bandwidth.

In fact, ESA matching with lossless inductors and capacitors is effective only over small bandwidths because the antenna impedance is not purely resistive. Indeed, ESA exhibits a high reactance value, which makes it difficult to be matched widely by only using passive matching. Moreover, Lopez [1] has explained the potential bandwidth improvement for various numbers of passive matching circuits, and concluded that adding one additional passive circuit will improve the bandwidth but in practice, most of the benefit is obtained by using one or two passive circuits, and a complicated matching circuit would contain substantial losses. All these facts limit the gain in bandwidth that passive matching can achieve.

On the other hand, non-Foster elements allow greater matching bandwidth compared to passive matching [12]. In non-Foster matching, lossless impedances that violate the Foster theorem [13] are used. In non-Foster components, the derivative of the impedance with respect to frequency is negative, meaning that its reactance-versus-frequency slope is negative. For that reason, using non-Foster matching can overcome the restrictions of gain-bandwidth theory that restrict passive matching.
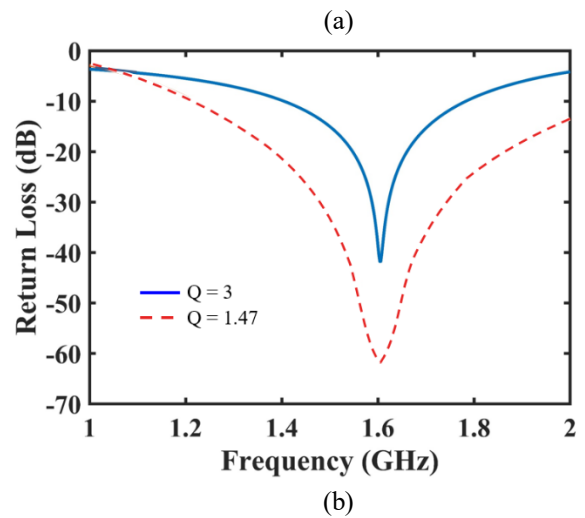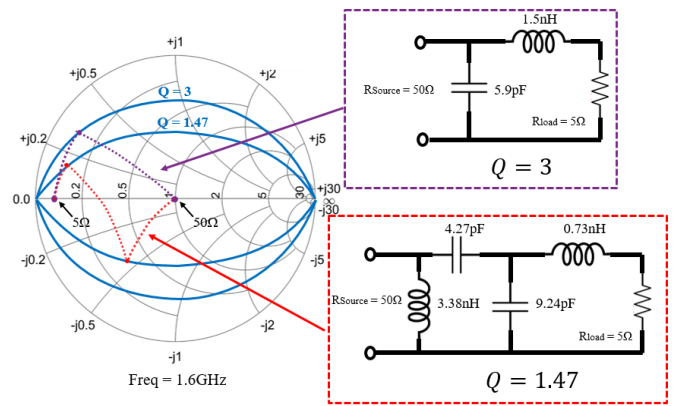

(a)

(b)

Fig.4 Comparison between 1 stage L-network and 2 stage L-network on Q factor (a), the effect of Q factor on bandwidth for a 5Ω load.

Non-Foster element usefulness relies on its negative reactance slope, because this property causes the corresponding impedance locus to proceed counter clockwise with increasing frequency. Figure 5 illustrates the classical ideal negative capacitor response and how it perfectly cancel a positive capacitance C of an antenna, over all frequencies, whereas the usual method uses a positive inductor L results in a single frequency matched point.
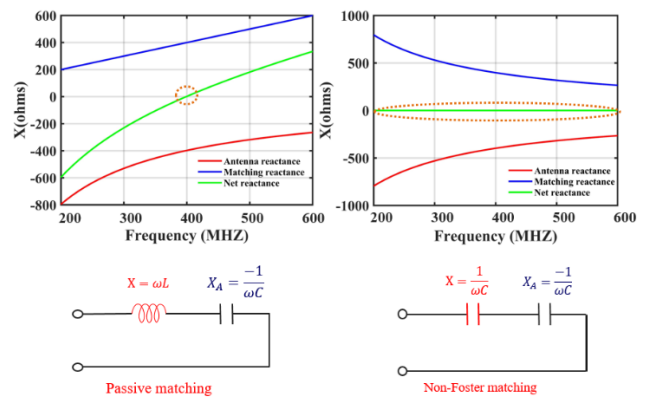

Fig. 5 Comparative concept of passive and NF matching for an ESA modeled by a series capacitor.

Typically, non-Foster Circuit (NFC) elements are negative capacitors and negative inductors that can be realized by using negative impedance converters or inverters (NICs or NIIs) [14]. However, relying only on NF elements to cancel the antenna reactance part is not sufficient to match the whole system, especially because the antenna real part is very low and far from 50Ω at lower frequencies. Therefore, a complementary passive matching network is usually added along with NF elements in order to move the net input impedance of the whole system to 50Ω.

In the upcoming sections, three topologies that combine NF and passive matching in different order are studied and applied to the monopole antenna and compared in terms of bandwidth and efficiency.

2.3 First matching topology: NF-Passive-Antenna

As illustrated by the blue curve in Figure 6 on Smith Chart, NF matching can be used to cancel the reactive part of the antenna but is not sufficient for our antenna to be matched in a frequency range from 1.5 to 1.7 GHz. Indeed, the net impedance is far from the goal of VSWR less than 2 (indicated by the light blue circle in Figure 6). VSWR is defined by:

$$VSWR = \frac{1 + |S_{11}|}{1 - |S_{11}|} \qquad (3)$$

Where S_{11} lower than -10 dB corresponds to VSWR less than 2, then any impedance within that 2-VSWR circle will lead to a power emitted from the source delivered to the load with a very little portion back scattered (10%). Therefore, to match the antenna, an increase of the real part is required. Figure 7 shows the real-part circles on Smith Chart with three different colored areas: red region corresponds to a real part between 0 and 25Ω, the green region between 25Ω and 100Ω, while the yellow area has a real part between 100Ω and infinity.
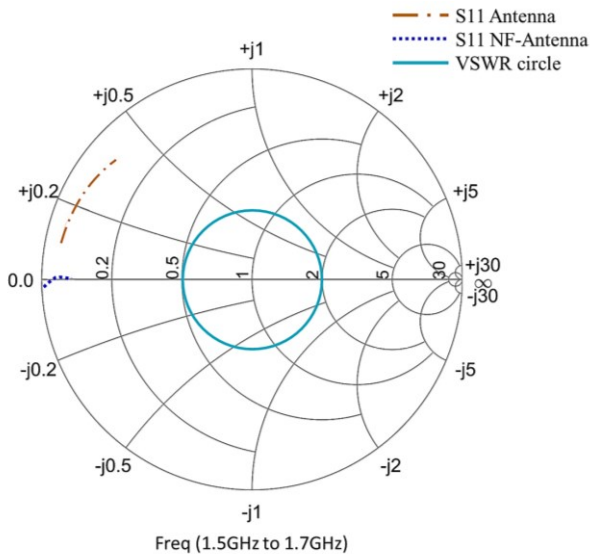

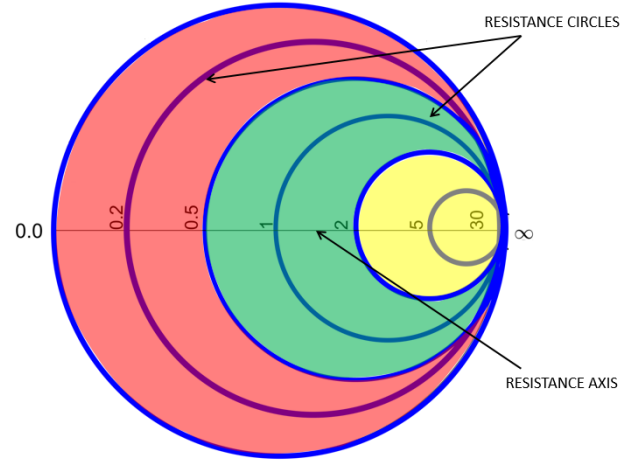**Fig. 6** Antenna matching on Smith Chart

Fig. 7 Resistance circles on Smith chart

If the antenna impedance gets inside the red region after using NF matching to cancel the antenna reactive part, a positive real resistor should be added in series to transform the net impedance within 2-VSWR circle to complete the matching process. Whereas, for an antenna impedance inside the yellow region, a negative resistance should be added in series to transfer the net impedance within 2-VSWR circle after canceling the reactive part. Adding a positive resistance is of course a wrong option, leading to power dissipation and less power delivered to the antenna, and consequently the radiation efficiency of the whole system will decrease. On the other hand, adding a negative resistance is also not preferable, because negative resistors are usually associated with a frequency dependent imaginary part, which in term will affect the matching bandwidth of the antenna. Finally, only the green area turns out to be relevant. Therefore, this requires transferring the antenna impedance inside the green region, and it can be done by using a transformer as seen in Figure 8-a, the values of the transformer are obtained by optimization in order to get a wide range of the antenna real part inside the green region (red curve in Figure 9). Then, NF matching is used to transfer the new impedance inside the 2-VSWR circle (yellow curve in Figure 9). It can be noticed that canceling the reactance part of the antenna associated with transformer system requires a parallel negative capacitance and negative inductance in series with a negative capacitance and negative inductance as seen in Figure 8-b. Their values were also optimized and the step-by-step matching process is shown in Figure 9 on Smith Chart.
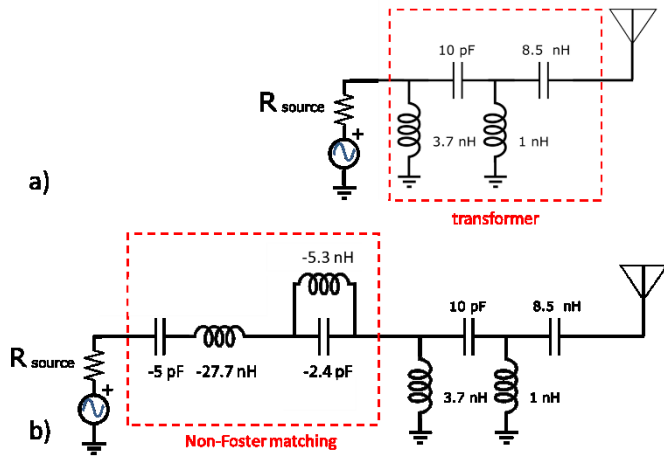
Fig. 8 Antenna with Passive transformer (a), antenna with NF-Passive matching (b)
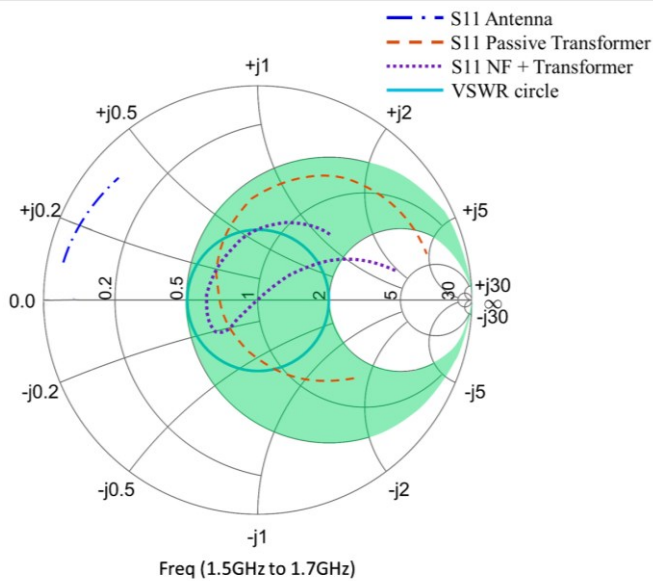
Fig. 10 (a) One stage L passive matching (b) two stages L matching (c) three stages L matching

Fig. 9 Antenna matching steps on Smith Chart
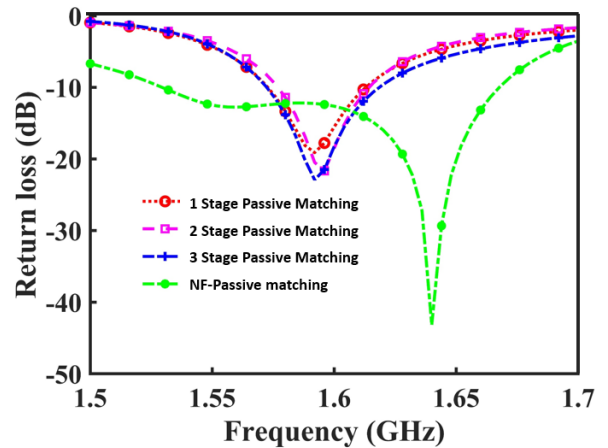
Fig.11 Multi-stage passive L-networks vs NF and passive matching

At this stage, a comparison between this topology and a conventional multistage passive matching is carried out to illustrate the bandwidth enhancement and matching improvements: 1 stage, 2 stages and 3 stages L-networks are used to increase the matching bandwidth of our antenna at low frequency range as seen in Figure 10. The values of the multistage passive elements are optimized to get an optimum return loss. As expected, Figure 11 illustrates that using NF combined with passive matching provides a wider bandwidth compared to classical multistage passive matching, which confirms that NF matching can overcome the gain bandwidth limitation of ESAs.
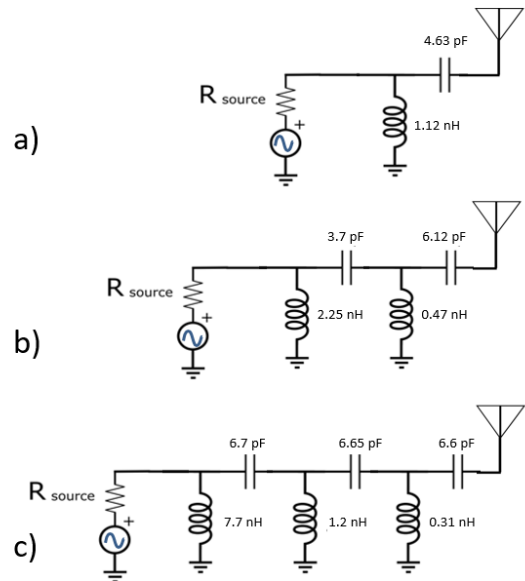
This topology is limited by how much bandwidth of the antenna impedance can be transferred within green area through passive matching, and how much active matching can cancel the reactive part to push the net impedance inside 2-VSWR circle. To overcome these limitations, a 2nd topology that combines NF and passive matching in a different order [10], [11] is put forward in next section.

2.4 Second matching topology: Passive-NF-Antenna

As previously mentioned, multistage L-section passive matching is one of the simplest ways to widen the bandwidth of any load, but this method is efficient for purely resistive load, i.e. with null reactive part. However, ESAs impedance includes a high reactance part and a low real resistive part. Thus, the design procedure described here consists in canceling first the load reactance part and then matching the remaining resistive part to 50Ω by using multi-stage passive network, in order to get a wide matching performance.

Canceling the reactance of the antenna will lead to lowering the Q factor (Equation 4). The system Q factor is given by the following expression:

$$Q = \frac{Im(Z_{matching\ circuit}) + Im(Z_{antenna})}{Re(Z_{matching\ circuit}) + Re(Z_{antenna})} \quad (4)$$

When $Z_{antenna}$ is reduced or compensated by $Z_{matching\ circuit}$, the Q factor decrease, leading to an increase in the bandwidth according to Bode criterion [7] expressed as follows:

$$\frac{\Delta f}{f_0} \leq \frac{\pi}{Q \ln(1/\Gamma_m)} \quad (5)$$

Where Γ_m is the desired reflection coefficient of the antenna at its input port, and f_0 and Δf are the central frequency and bandwidth respectively. In order to identify and quantify the antenna reactance to be canceled, we search first for the antenna low-frequency equivalent model (i.e. an inductor with a capacitor and a resistor in series Figure 12-a). Its reactance part is compensated by NF part, leaving only net real impedance. The next step consists in using passive transformer to transform the net impedance to 50Ω (Figure 13). The values for passive transformer were optimized by targeting a wide matched bandwidth. Figure 14 present the overall return loss obtained by this method.
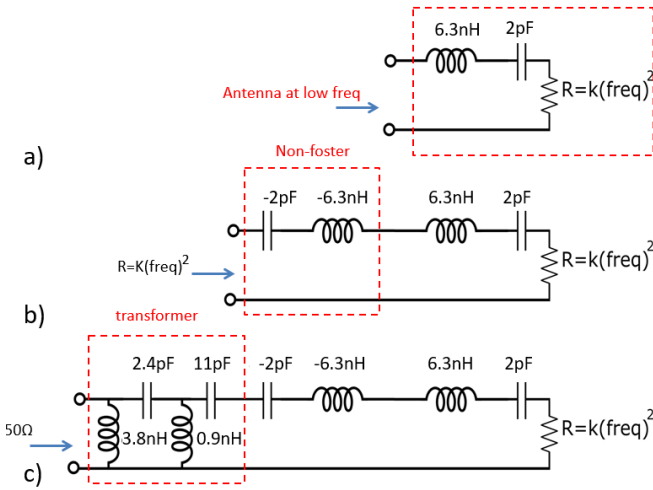

a)

b)

c)

Fig. 12 Antenna model at low frequency (a), NF reactive part compensation (b), complete matching (c)
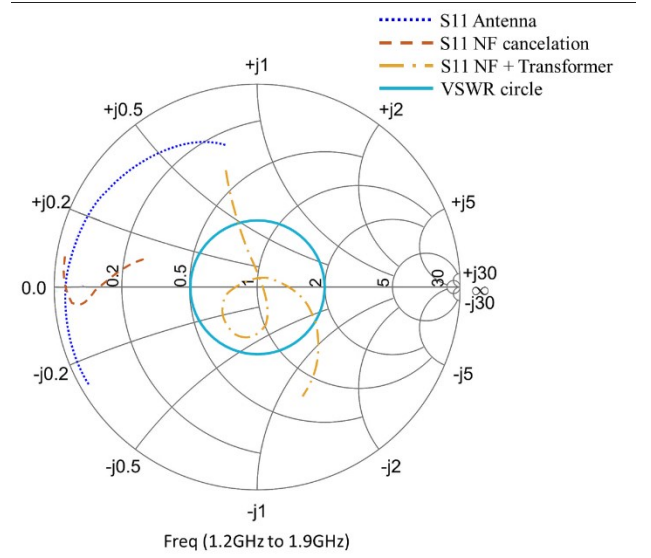

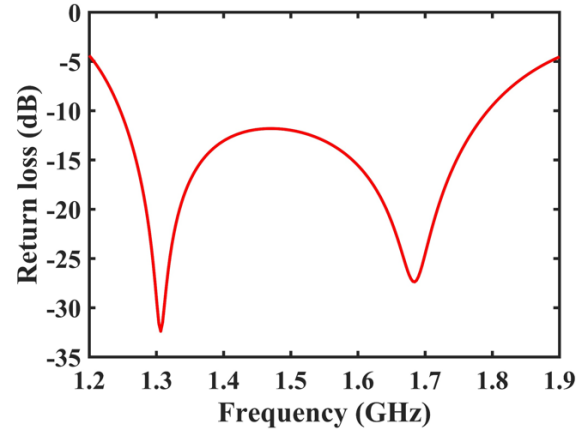**Fig. 13** Passive-NF matching on Smith Chart

Fig. 14 Passive-NF matching

The limit of this topology relies on how much and over which bandwidth can NF matching cancel the antenna reactive part which further allows the complementary task of passive matching to be effective. Moreover, decreasing the Q factor of the circuit in order to get a wide matching bandwidth still require multistage of L-networks. The third topology merges the first two topologies advantages and allows better performances in terms of matching bandwidth and efficiency.

2.5 Proposed matching topology: Passive-NF-Passive-Antenna

This proposed topology aims first to decrease the antenna Q factor by using passive matching, i.e. by increasing the antenna resistive part, second cancel the reactive part by introducing NF matching leading to decreasing more the Q factor and finally shift the input impedance to 50 Ω by using passive matching. The topology steps are shown in Figure 15 and the corresponding impedances are plotted step-by-step on Figure 16.
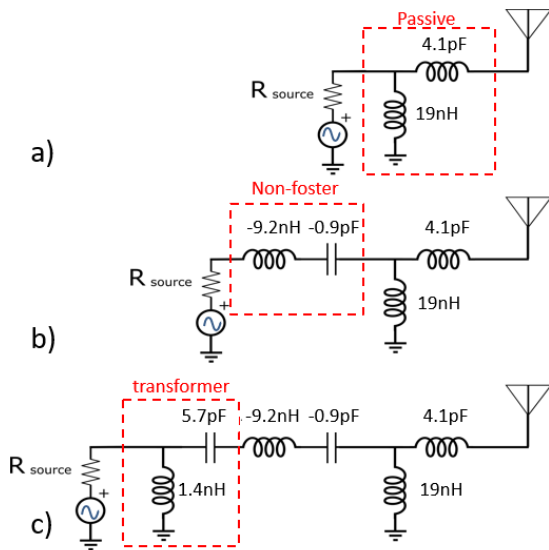
Fig. 15 Illustration of the step-by-step matching using the 3rd topology (a) Passive matching, (b) Non-Foster matching, (c) Passive transformer

It can be noticed that by using first a passive matching circuit the antenna real part is increased by only 5Ω, because a larger increase will make it more difficult for active matching to cancel its reactive part. Furthermore, the effect of the second step (NF canceling) is clear in Figure 16 as the input impedance curve gets close to the real axis of the Smith Chart .Finally, an L-section passive circuit shifts this impedance inside the 2-VSWR circle.
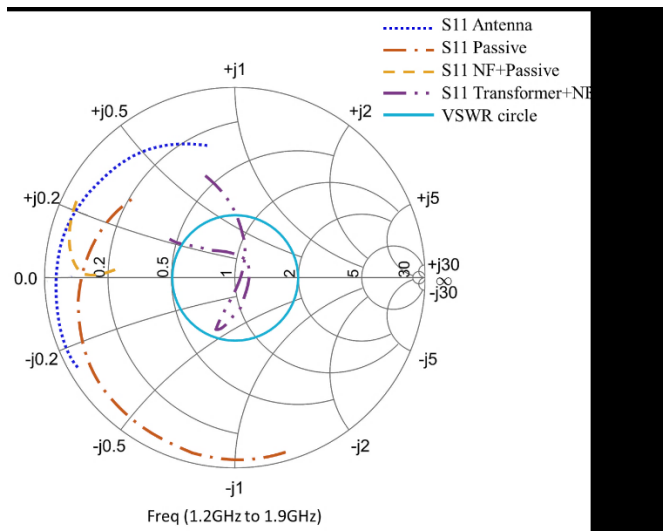

Fig. 16 Step-by-step wideband matching for the 3rd topology

A comparison of the return loss between our proposed topology and the previously described ones is shown in Figure 17. Our topology extends the bandwidth towards a lower frequency range by merging the first two techniques together, i.e. it changes the antenna real part and cancels the reactive part like the first topology, and then it transfers the net impedance toward 50 Ω just like the second topology.
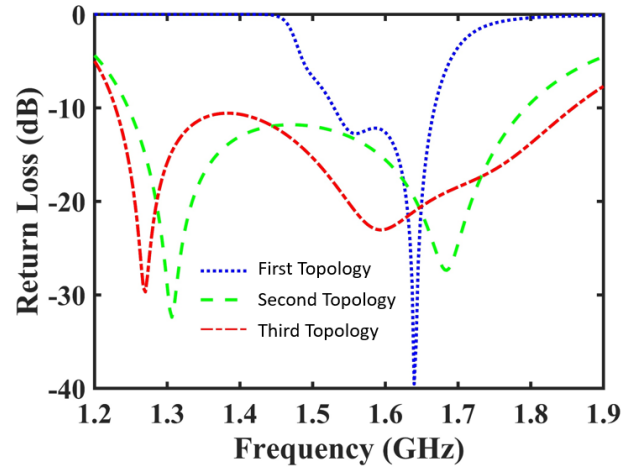

Fig. 17 Comparison of the return loss from the three topologies

These steps affect the Q factor of the whole matching network, which leads to a lower value compared to the first two topologies as shown in Figure 18. The quality factor is thus defined as the absolute ratio of the net reactance of the matching system to the ratio of its real part. Note that Q-plot agrees perfectly with the return loss graph. In addition, Table 1 shows the comparison between the fractional bandwidth of the three topologies and the conventional passive matching and it confirms that our proposed topology gives a wider bandwidth response compared to other matching topologies.
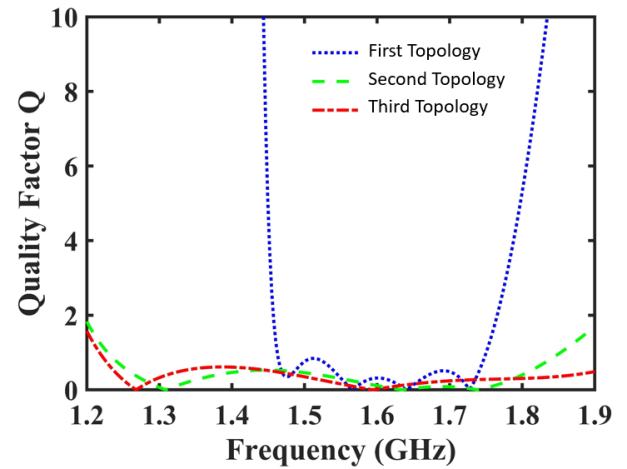
Fig. 18 Comparison between Q factor of the whole matching network of the three topologies

Table 1 Bandwidth comparison between different matching topologies

Topology	Bandwidth	Fractional Bandwidth
1 Stage Passive	0.028GHz	1.75%
2 Stage Passive	0.042GHz	2.62%
3 Stage Passive	0.061GHz	3.81%
First Topology	0.142GHz	8.87%
Second Topology	0.558GHz	37.2%
Third Topology	0.622GHz	41.46%

Our topology limits depend on how much a passive network can increase the resistive part of the antenna without making it difficult for NF matching to perfectly cancel the reactive part obtained after this transformation. Finally, antenna impedance matching (i.e. S_{11}) provides a necessary but insufficient information for the user, to ensure a satisfactory result; one should also calculate the efficiency of the whole system, which is done in the next section.

2.6 Topologies comparison and discussion

In this section, we aim to compare the performance in term of efficiency of the three topologies cited above. To do so, we can simulate each topology using CST, however it's a time consuming method and needs to be repeated at each frequency in the considered bandwidth. Thus, in order to simplify that and have a better knowledge about power consumption, we suggest the introduction of a factor called Total Transmission Coefficient (TTC), which is the ratio of the delivered power to the antenna over the provided power by the source Equations (7) and (8) (Figure 19). By calculating TTC we can have an idea about the efficiency of the whole system including the antenna without the need to simulate the antenna with the matching circuit with time consuming EM software (e.g. CST or HFSS software). So this way we can do an optimization in order to increase the antenna efficiency and bandwidth by only focusing on using ADS software.

This factor gives a rough value of the radiating efficiency of our system, which is defined as the ratio of the effective radiated power (except for internal antenna losses and energy stored in its near field) to the input power of the source as Equation (6):

$$Eff\ Radiated = \frac{Power\ Radiated}{Power\ Incident} \tag{6}$$

TTC can be expressed as:

$$TTC = \frac{\sqrt{|b_2|^2 - |a_2|^2}}{\sqrt{|a_1|^2}} \tag{7}$$

$$TTC = \frac{\sqrt{|S_{21}|^2 * (1 - |\Gamma_{load}|^2)}}{|1 - S_{22} * \Gamma_{load}|^2} \tag{8}$$

If our matching circuit is perfectly lossless and the load (i.e. the antenna) is perfectly matched, then the TTC factor must be equal to one (a_2 = zero, and $b_2 = a_1$), meaning that the maximum incident source power is all transmitted to the load.
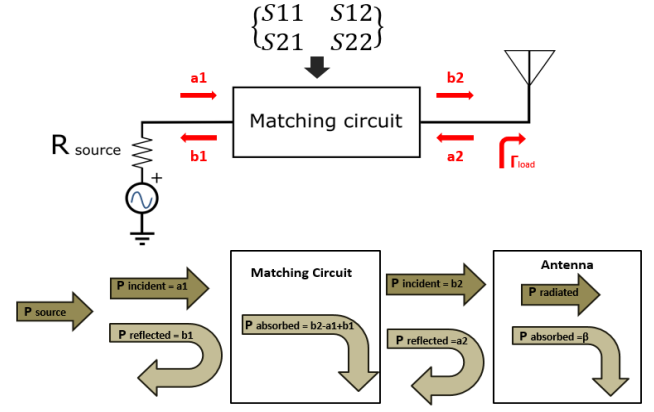

Fig. 19 Incident and reflected waves at the matching circuit accesses

Figure 20 shows the calculated TTC of the three topologies. We can notice that using our proposed 3-stage matching network provides a better result than the other two topologies. It must be noted that the radiated efficiency and TTC are related together by the following equation:

$$Eff\ Radiated = TTC - \beta \tag{9}$$

Where β accounts for the power absorbed inside the antenna, which can be divided in two parts: the first part is the loss resistance that transforms power into heat and the other part stores the energy in its near field, which relies to the antenna reactive part [15]. Regardless of the power loss, by calculating TTC we can know how much power is delivered to the antenna input from how much power is absorbed or reflected back by the matching circuit.
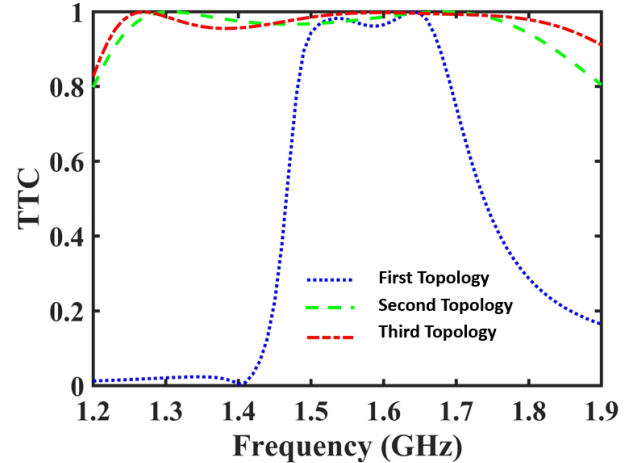

Fig. 20 Comparison of TTC for the three topologies

Co-simulations between ADS and CST software have been done (Figure 21) in order to measure the matched antenna radiating efficiency and compare it with TTC for the three topologies. It can be noticed that the three curves of the matching topologies follow the curve of the maximum achievable radiated efficiency of the antenna at lower frequency, which validate our TTC results about the power being all delivered to the input port of the antenna. Toward low frequencies, only a portion of power is radiated as illustrated by radiation efficiency whatever the matching network. Indeed, as we go lower in frequency the expected

radiation efficiency of the antenna decreases, and that is related to the increase in the antenna Q factor, which in term means that losses inside the antenna will increase strongly at lower frequency. In other word, it is useless to match the antenna at very low frequency, because the power that is going to be delivered at the antenna input port would be dissipated inside the antenna or even stored in its near field, while a very low percentage will be radiated.
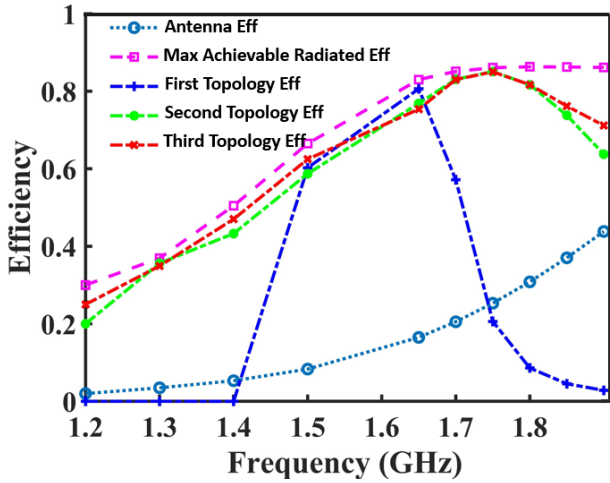

Fig. 21 Efficiency of the system

3 NF circuit design, actual implementation and measurements

In this section, we present the actual implementation of the two matching topologies (Second topology and third topology). Figure 22 shows the circuit layouts and the corresponding photos. Calibrated Measurements were conducted with the aid of Rohde & Schwarz ZNB-20 VNA in our laboratory but the measurement setup was not placed in an anechoic chamber.

In addition, Figure 23 shows a schematic view of the two topologies. Linville cross-coupled pair (XCP) of FETs with output on sources (also called open circuit stable OCS [16]) was selected due to its potential wideband NF behavior and because after a thorough stability analysis it was found to be easier to stabilize than XCP with output at drains (also called short circuit stable SCS [16]). We have chosen SKY65050 transistor from Skyworks for our NF circuit. All the elements used for passive and NF matching are depicted in Figure 23 including biasing network, whereas the element values are summarized in Table 2.
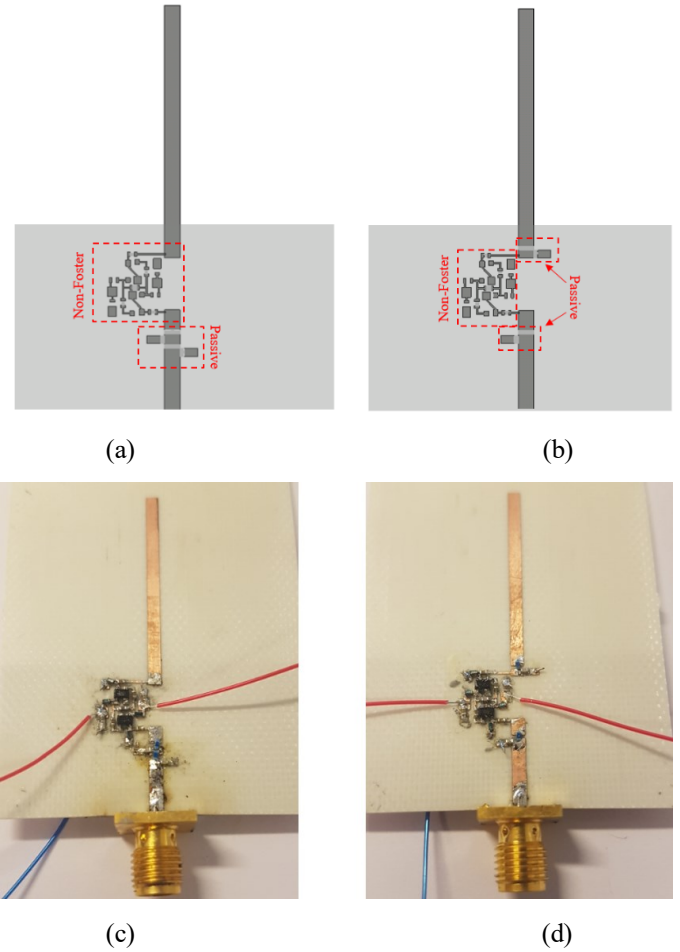

Fig. 22 Combined passive and NF matching networks: second topology (a), third topology (b), and respective photos (c), and (d)

It must be noticed that in both topologies, we only use a negative capacitance instead of –L and –C in simulation. This was done for simplification purpose and because the equivalent model of the antenna at low frequency corresponds mainly to a capacitance behavior (Figure 2). Measurement results are presented on Figure 24 and compared to complete simulations, including FET S-parameters, lines sections and bias networks influence. It can be noticed that both topologies have a wideband matched response with a rather good agreement between simulated and measured results and that the bandwidth widening obtained from the third topology is confirmed.
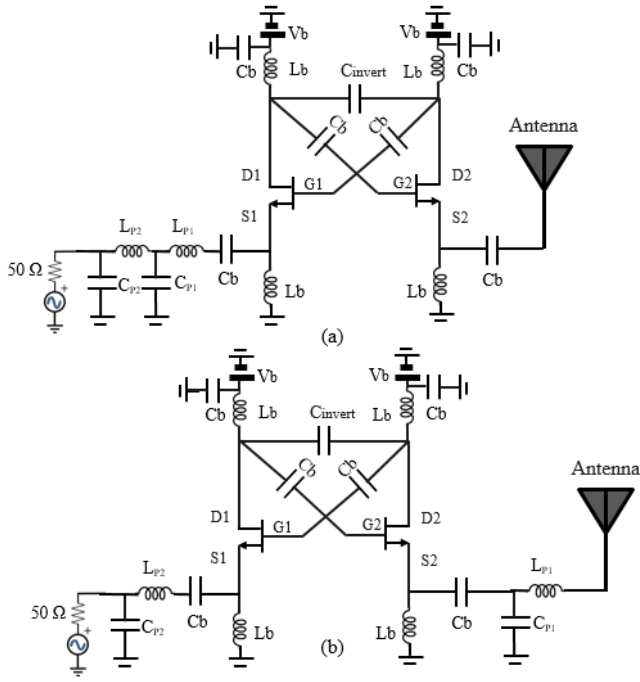
Fig. 23 Schematic of combined Passive and NF matching, second topology (a), and third topology (b)

Table 2 Component values used in both topologies of combined passive and NF matching

Components	C_{invert}	C_{p1}	C_{p2}	L_{p1}	L_{p2}
Topology one	2pF	0.8pF	0.6pF	2.5nH	1nH
Topology two	3pF	0.6pF	0.5pF	0.7nH	0.5nH

Unfortunately, in both cases, it is also partly due to the residual real part introduced by NF circuit, which slightly improves the matching response. Indeed, the implemented NF circuit does not provide a pure negative capacitance, it introduces a negative capacitance but with a residual positive real part [17], which in term dissipates energy resulting in a wider matched band. This phenomenon is already evidenced while comparing simulations from ideal components of Figure 17 and the most complete ones of Figure 24 that include this spurious resistive part.

The effect of residual positive real part can be shown when calculating the TTC of both topologies. Figure 25 presents a comparison in TTC between the two topologies together with the whole systems efficiencies. It can be notice that TTC is not equal to one as experienced when using ideal negative elements, which indicates that the matching network absorbs a portion of the incident power, thus lowering the total efficiency of the system as seen in Figure 25. This residual part was estimated at about 23Ω, close to $2/g_m$ (g_m is the FET transconductance).

At this stage, it is important to estimate the relevance of these results compared to previous studies. First, few actual implementations of NF circuits associated with measurements are provided above 1 GHz, probably because of stability issues and spurious effects (e.g. parasitic capacitances of the transistors, interconnect lines inside the XCP) that degrade the expected NF response. Moreover, very few of them had mentioned the system efficiency

mainly because getting a stable response together with a low residual resistive part and a sufficient negative capacitance value (of the order of pF or hundreds of fF) is particularly tricky above 1 GHz.

Nevertheless, several ways could be explored to face out this resistive part issue:

- First, as put forward in [17], XCP-source topology can be cascaded by XCP-drain one to compensate each other their real parts but stabilizing drain topology remains challenging and the whole system requires twice as many transistors.

- Negative Group Delay (NGD) circuit could be used to generate negative reactance [18], [19] response but over narrower frequency band because they are mainly based on resonant behavior. Moreover, NGD is always associated with losses that should be compensated by amplifiers.

- Integrated technologies (MOS, Bi-CMOS) could be used to NF circuit design to get a high transconductance value for the transistor to lower the residual resistive part. Cascode FET topology [20] could also be tried to increase the transconductance and thus reduce the resistive residual part, but again at the expense of the number of transistors.
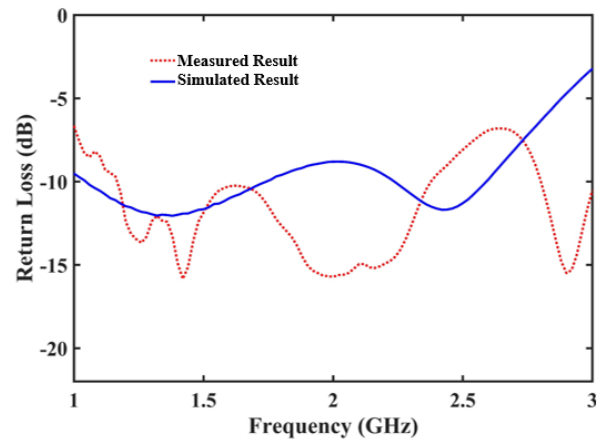
(a)
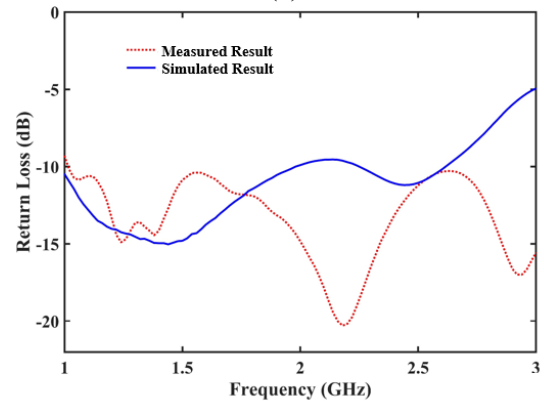
(b)

Fig. 24 Simulated vs Measured Results of Passive NF matching of second topology (a), and third topology (b)
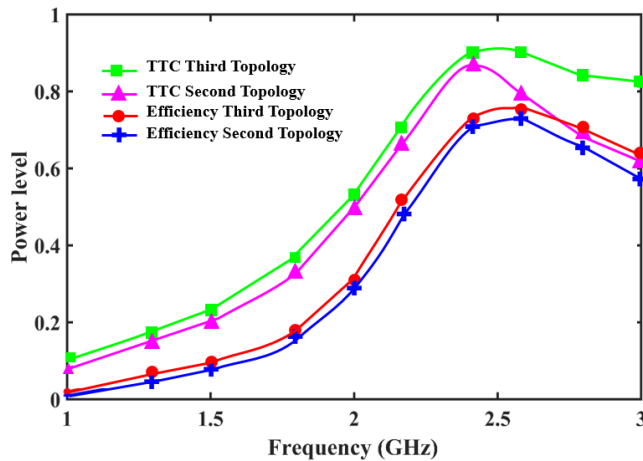
Fig. 25 TTC and Efficiency comparison between second and third topology

4 Conclusions

A detailed matching methodology has been carried out on three different matching topologies that use NF and passive elements. These matching topologies were applied to match a planar monopole antenna at low frequency band over a wide band, i.e. creating a wideband ESA. The first topology uses passive then NF matching network, while the 2nd topology uses NF and then passive network to match the antenna at low frequency band. In both cases, multistage passive networks can be introduced to improve the bandwidth by decreasing the Q factor but at the expense of losses in practical implementations. The 3rd proposed approach is introduced in this paper and combines the two previous topologies by focusing on decreasing the Q factor, which is done by first increasing the real part of the antenna using passive transforming, after that canceling the reactive part using NF elements, and finally passive matching is used to transfer the impedance toward 50 Ω. We have also introduced and simulated TTC (Total Transmission Coefficient) parameter in order to estimate, without the need to simulate the whole circuit in CST or HFSS software, the power actually radiated by the antenna when using these three types of matching networks. The obtained results shows that the proposed topology (3rd topology) has a wider bandwidth and better radiation efficiency compared to the other two networks. Finally, practical implementations are presented and measurements (i.e. using non-Foster) are compared to simulation results for both second and third topologies.

References

1. A. R. Lopez, "Review of narrowband impedance-matching limitations," *IEEE Antennas Propag. Mag.*, vol. 46, no. 4, pp. 88–90, Aug. 2004.
2. M. M. Jacob, J. Long, and D. F. Sievenpiper, "Broadband non-Foster matching of an electrically small loop antenna," in *Proceedings of the 2012 IEEE International Symposium on Antennas and Propagation*, 2012, pp. 1–2.
3. Y. Xia, Y. Li1, S. Zhang, "A Non-foster Matching Circuit for an Ultra-wideband Electrically Small Monopole Antenna",13ᵗʰ European Conference on Antennas and Propagation (EuCAP 2019)
4. L. J. Chu, "Physical Limitations of Omnidirectional Antennas Physical Limitations of Omnidirectional Antennas."
5. A. D. Yaghjian and S. R. Best, "Impedance, bandwidth, and Q of antennas," in *IEEE Antennas and Propagation Society International Symposium. Digest*, 2003, vol. 1, pp. 501–504 vol.1.
6. H. A. Wheeler, "Fundamental Limitations of Small Antennas," *Proc. IRE*, vol. 35, no. 12, pp. 1479–1484, Dec. 1947.
7. H. W. Bode, *Network Analysis and Feedback Amplifer Design*. New York: Van Nostrand Company, 1945.
8. R. M. Fano, *Theoretical limitations on the broad-band matching of arbitrary impedances*, vol. 249. J. Franklin Inst., 1950.
9. D. F. Sievenpiper *et al.*, "Experimental Validation of Performance Limits and Design Guidelines for Small Antennas," *IEEE Trans. Antennas Propag.*, vol. 60, no. 1, pp. 8–19, Jan. 2012.
10. N. Ivanov, B. Buyantuev, V. Turgaliev, and D. Kholodnyak, "Non-foster broadband matching networks for electrically-small antennas," in *2016 Loughborough Antennas Propagation Conference (LAPC)*, 2016.
11. M. Manoufali, Abbosh "Non-Foster Impedance Matching of an Electrically Small Loop Antenna for Biomedical Telemetry", IEEE Asia Pacific Microwave Conference 2017.
12. S. Koulouridis, M. Livadaru, and J. L. Volakis, "Antenna minimization with active and passive matching circuits," in *2008 IEEE Antennas and Propagation Society International Symposium*, 2008, pp. 1–4.
13. R. M. Foster, "A reactance theorem," *Bell Syst. Tech. J.*, vol. 3, no. 2, pp. 259–267, Apr. 1924.
14. J. G. Linvill, "Transistor Negative-Impedance Converters," *Proc. IRE*, vol. 41, no. 6, pp. 725–729, Jun. 1953.
15. "Antenna Efficiency." [Online]. Available: http://www.antenna-theory.com/basics/efficiency.php. [Accessed: 01-Oct-2019].
16. J. Brownlie, "On the Stability Properties of a Negative Impedance Converter," IEEE Trans. Circuit Theory, vol. 13. no. 1, pp. 98–99, Mar. 1966.
17. Saadou Al Mokdad, Raafat Lababidi, Marc Le Roy, Sawsan Sadek, André Perennec, Denis Le Jeune, "Wide-band Active Tunable Phase Shifter Using Improved Non-Foster circuit" *IEEE International Conference on Electronics, Circuits and Systems (ICECS)*, Dec. 2018.
18. B. Ravelo, A. Perennec, M. Le Roy, and Y. G. Boucher, "Active microwave circuit with negative group delay," *IEEE Microw. Wireless Compon. Lett.*, vol. 17, no. 12, pp. 861–863, Dec. 2007.
19. H. Mirzaei and G. V. Eleftheriades, "Realizing Non-Foster Reactive Elements Using Negative-Group-Delay Networks," *IEEE Trans. on Microwave Theory and Techniques*, vol. 61, no. 12, pp. 4322-4332, Dec. 2013.
20. L. Batel, L. Rudant, J.F. Pintos, K. Mahdjoubi, "Réseau d'antennes compact, super directif et large-bande associé aux éléments Non-Foster", *JNM Saint-Malo*, France, 2017.